

**Simulating Field Conditions for the Curing of Saltstone – 15501**

Steven Simmer \*, Ian L. Pegg \*\*

\* Savannah River Remediation, LLC

\*\* Vitreous State Laboratory, The Catholic University of America

**ABSTRACT**

Saltstone is a cementitious, low-level waste (LLW) material processed and stored at the Savannah River Site (SRS). It consists of fly ash (FA), blast furnace slag (BFS), and Portland cement that are blended with LLW salt solution. The dry feed materials and the salt solution are mixed at the Saltstone Production Facility (SPF), and the fresh grout subsequently pumped into a Saltstone Disposal Unit (SDU) in the Saltstone Disposal Facility (SDF) where it cures to form a rigid, cementitious monolith. In order to demonstrate the long-term performance of saltstone, non-radioactive simulant samples are processed and cured in a laboratory environment and subsequently tested with respect to key performance properties. Of particular relevance to assessing the long-term stabilization and immobilization of radionuclides in saltstone is the permeability, or saturated hydraulic conductivity, which determines the rate of infiltration for oxygen-bearing ground waters that can affect redox sensitive contaminants, such as <sup>99</sup>Tc.

Environmental conditions in the SDU, in particular temperature and humidity, are believed to affect the cured properties of saltstone. With respect to humidity it has been determined that the average vapor space humidity in an SDU is at least 95%, and in addition the assumption can be made that underlying grout is subjected to a moisture-saturated environment by the grout poured over it. With respect to temperature, the SDUs contain thermowell arrays that provide detailed vertical, and to a lesser degree radial, temperature profiles. Temperature data from the SDUs have subsequently been utilized to better simulate curing temperatures for simulant saltstone in the laboratory. However, no two thermal profiles are the same, varying with respect to the following parameters: initial temperature, rate of temperature increase, maximum temperature attained, time at maximum temperature, and cooling rate. These temperature variables are dependent on the depth of grout (due to insulating effects of underlying and overlying grout), frequency of grout addition to the SDU (with more frequent additions causing grout temperatures to rise due to the exothermic hydration reactions), and, to a lesser degree, the ambient temperature of the external environment.

Due to the variability in each thermal profile recorded in an SDU, the question arises as to which profile (or profiles) should be used in the simulated laboratory environment to best mimic the curing of field emplaced saltstone, such that there is confidence that the properties measured for laboratory-prepared samples are representative of the grout in the SDU. Since the current SDU design contains sixty-six thermowells it is obviously not practical to process simulant samples according to each profile. Rather the aim would be to choose a reduced number of profiles that adequately encompass the range of recorded profiles, or to choose a single profile that is considered most conservative with respect to the resulting properties of interest. This is typically thought to be the profile exhibiting the highest peak temperature since for cement-based materials higher curing temperatures (> 60 °C), while resulting in enhanced reaction kinetics and strength development for short curing durations (~28 days), have been shown to adversely affect the physical properties of the material after extended cure times. In choosing representative profiles it is important to consider not only the maximum temperature, but also the influence of rate of temperature rise to the maximum temperature, and time at or close to the maximum temperature on the post-cured properties.

The intent of this paper is to consider the varied curing temperature profiles to which the saltstone is exposed in an SDU, and to analyze the currently available data for elevated temperature curing of saltstone to determine the potential thermal effects on the saturated hydraulic conductivity of saltstone emplaced in an SDU. This may subsequently facilitate a more informed approach to simulating the curing of saltstone in a laboratory environment.

## INTRODUCTION

Saltstone is a cementitious material utilized at the Savannah River Site (SRS) to encapsulate and immobilize low-level waste (LLW). Alkaline salt solution with an approximate free hydroxide concentration of 2 M [1] is mixed with a three component dry feed mixture consisting of ordinary Portland cement (OPC), blast furnace slag (BFS), and fly ash (FA). The dry feeds are mixed in a mass ratio of 45/45/10 BFS/FA/OPC and combined with the salt solution to achieve a water-to-cementitious materials (w/c) ratio of 0.6. The components are mixed in a high shear mixer in the Saltstone Production Facility (SPF) and ultimately transferred to a Saltstone Disposal Units (SDU) for long term storage.

In order to determine key physical and chemical properties of saltstone, non-radioactive simulant materials are prepared and cured in the laboratory. However, when preparing samples in the laboratory it is essential to simulate (to the extent practicable) the curing environment to which the field emplaced saltstone is subjected. In particular, relative humidity (RH%) and temperature have been shown to influence the cured properties of cementitious materials [2]; curing in low moisture environments can lead to plastic shrinkage cracking and reduced strength, whereas increased temperatures (around 50 °C) have been shown to initially increase the rate (and degree) of cement hydration and strength gain (e.g., 28-day cure) though as the curing duration increases both the degree of hydration and strength are degraded in comparison to samples cured at ambient temperature. Temperature and RH% are two variables that can be readily controlled in the laboratory. The RH% of the vapor space of an SDU has been measured over a period of 1 month and indicates that the average daily RH% was greater than 95% (Figure 1). In addition, it is relevant that this RH% is only applicable to the grout surface since it is assumed that the moisture content of underlying grout is maintained by the grout emplaced over it.

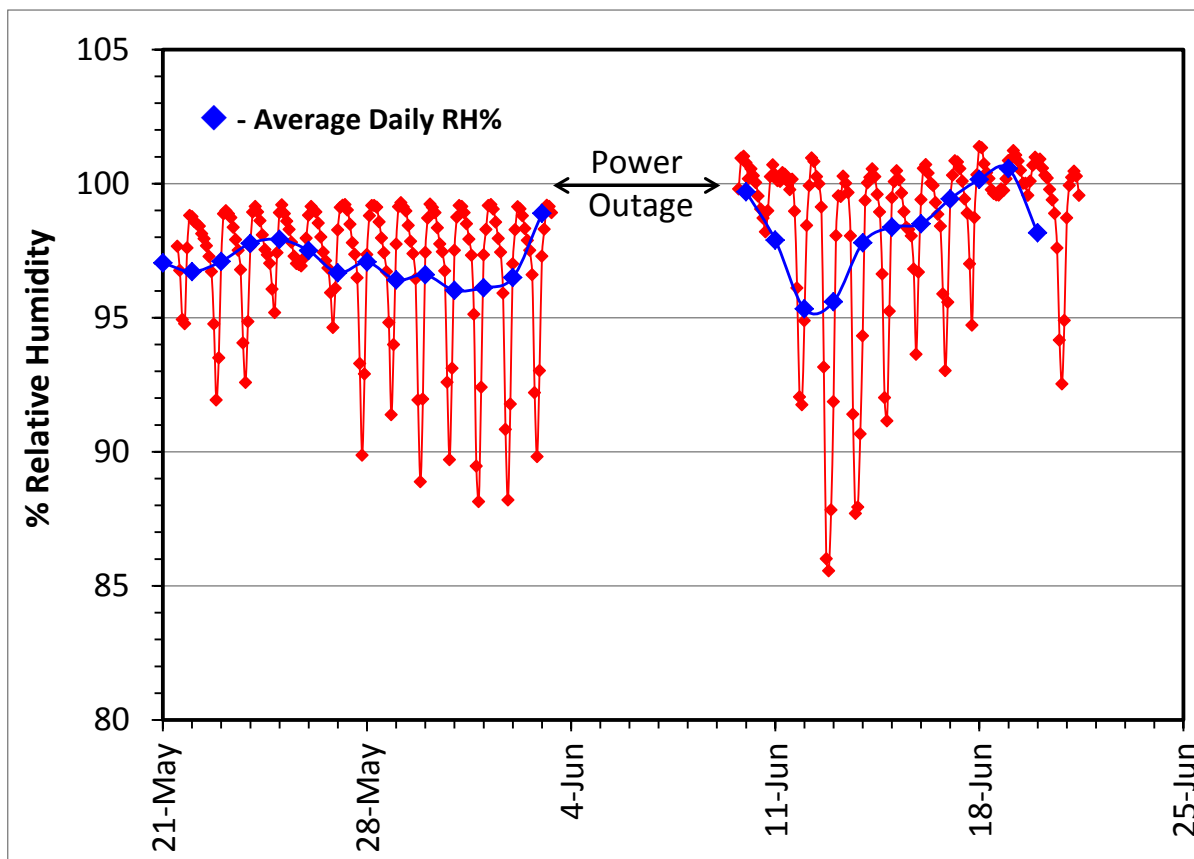


Figure 1: Relative humidity measured in an SDU (2013).

With respect to temperature, the SDUs incorporate three thermowell arrays (Figure 2) that provide detailed vertical thermal profiles at 30.5 cm (1-foot) intervals from 0.15 to 6.85 meters (0.5 to 22.5 feet) in the SDUs. One thermowell array is located at 3 meters (10 feet), and the other two, 15 meters (50 feet) from the SDU center.



**Figure 2:** Vertical thermowell array in SDU.

Figure 3 indicates the temperature recorded at an elevation of 2.9 meters (9.5 feet) in an SDU. The blue shaded region in the figure is associated with the time period before the 9.5-foot thermowell is covered with grout, and the temperature at this elevation is influenced by seasonal and diurnal changes in the ambient temperature in addition to radiant and convective heat transfer from grout lying below the 9.5-foot thermowell. Once the thermowell is covered with hydrating grout the temperature is significantly less sensitive to seasonal and diurnal changes in temperature.

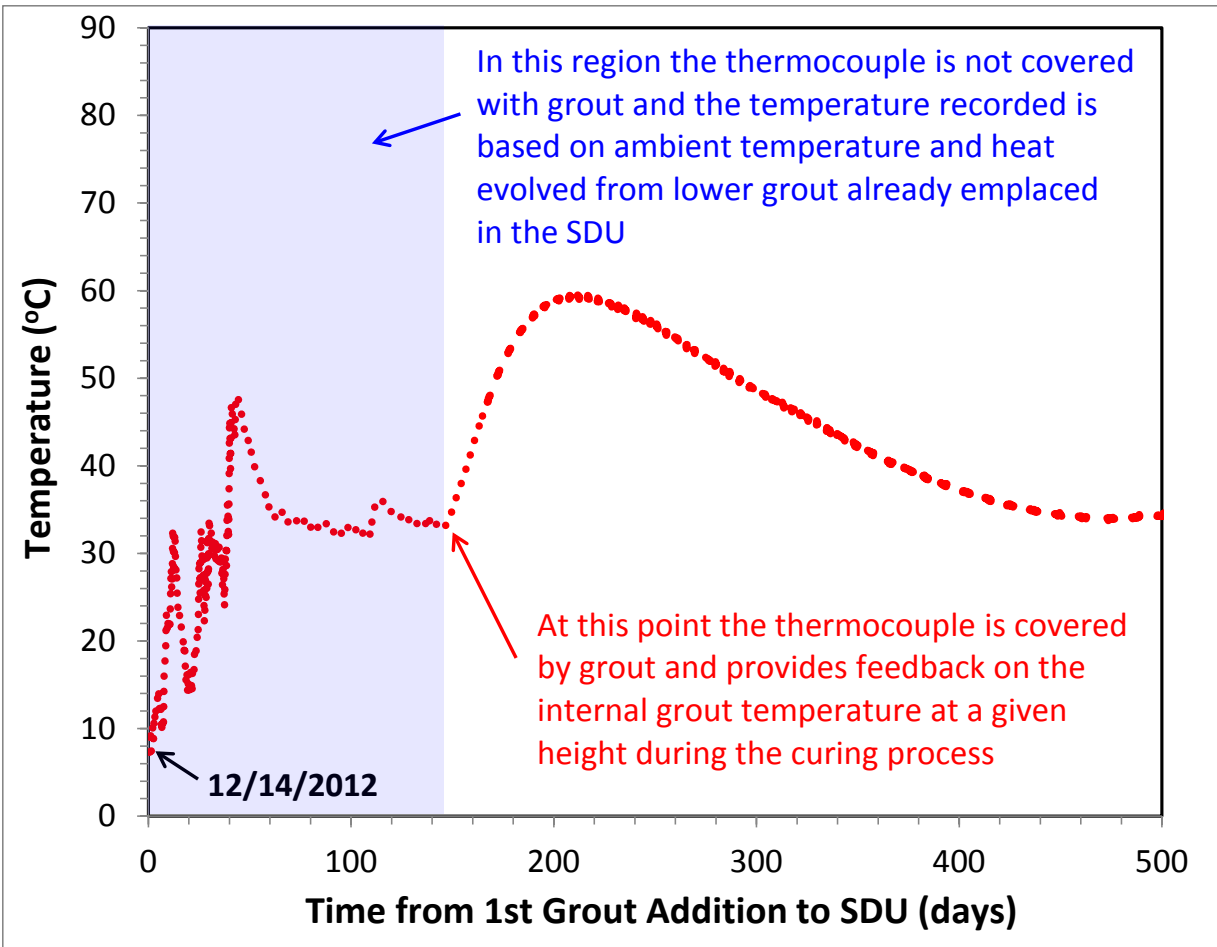


**Figure 3:** Example thermowell output at an elevation of 2.9 meters (9.5 feet) in SDU Cell 2A.

The approximate dimensions of currently utilized SDUs are 45.7 meters (150 feet) in diameter by 6.7 meters (22 feet) in height. Given the size of the SDU it is not surprising that significant variation exists with respect to the time-dependent thermal profiles at different locations in the SDU. These variations are influenced predominantly by the heat evolved during grout hydration, the insulating effects of the surrounding grout, and to a lesser degree by ambient temperatures; the former is dependent on the amount of grout poured into the SDU and the rate at which it is poured. Figure 4 shows an array of thermal profiles in an SDU from 0.46 to 4.7 meters (1.5 to 15.5-foot) elevations at 0.6-meter (2-foot) intervals. The start of each trace is associated with the time at which the thermowell (for a particular elevation) was covered with grout; time zero is the time that the 0.46 meter (1.5-foot) thermowell was initially covered with grout.

Figure 4 indicates that initial grout emplacement into this particular SDU began mid-December 2012. Grout emplacement continued for 2 months, was suspended for approximately 4 months, and then restarted. The figure indicates the disparity in the following thermal parameters for grout at the indicated elevations:

1. Initial temperature
2. Peak temperature
3. Rate of increase to peak temperature

4. Time at peak temperature
5. Rate of decline from peak temperature.

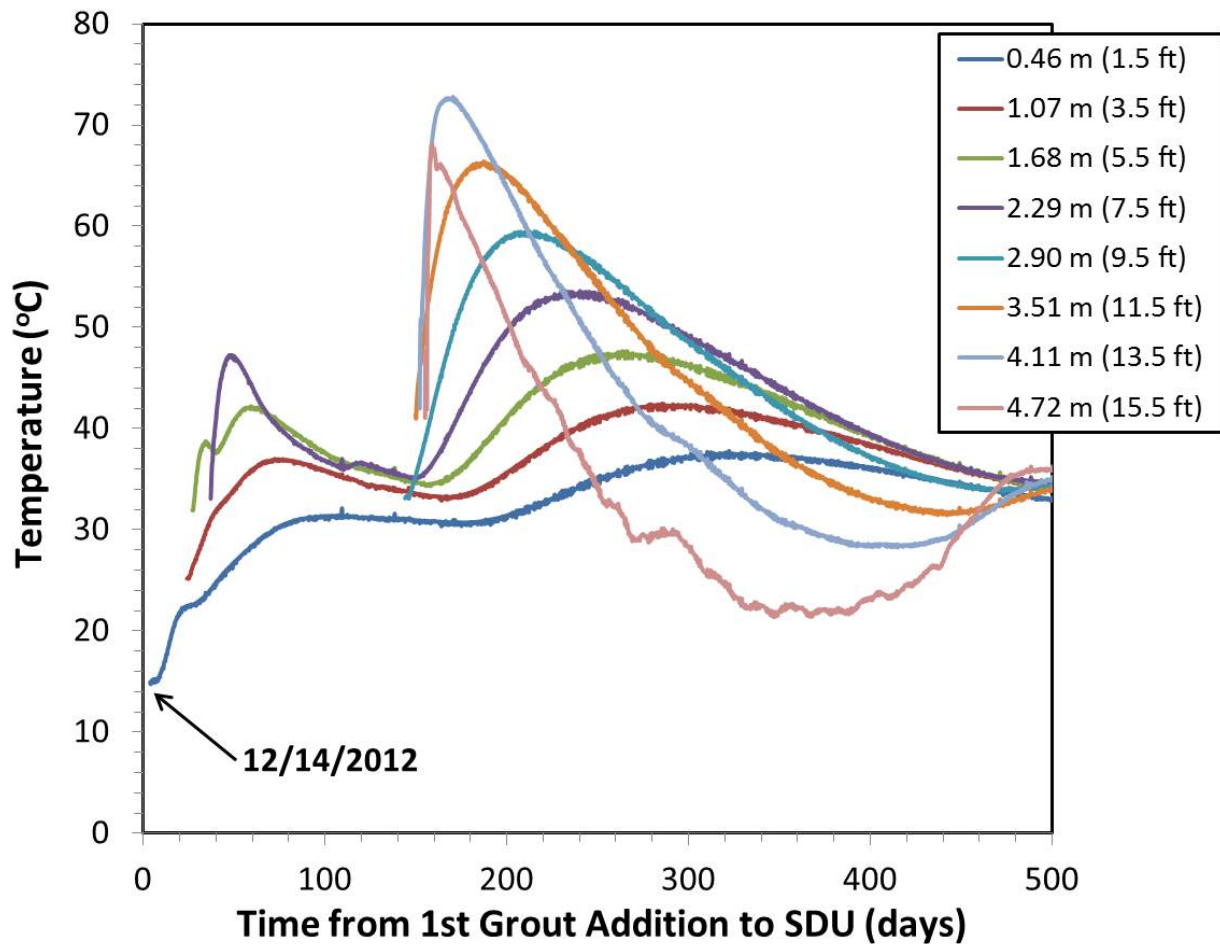


**Figure 4:** Thermocouple outputs for elevations from 0.46 to 4.72 meters (1.5 to 15.5 feet) in an SDU.

Figure 5 indicates the temperature profiles at each elevation during the first 90 days of grout curing at that particular elevation. In this figure time zero for each trace equates to the time at which a particular thermowell was covered with grout. To illustrate the variation in thermal history at different SDU locations consider the profiles in Figure 5 at 0.46 and 4.1 meters (1.5 and 13.5 feet). At the 0.46-meter (1.5-foot) elevation the initial temperature was 15 °C and the temperature gradually rose to 30 °C during the 90-day period. In contrast, the temperature of saltstone emplaced at the 4.1-meter (13.5-foot) elevation started at around 40 °C and increased to approximately 75 °C in less than 10 days. Not surprisingly, the length of time for which the peak temperature is maintained is less for grout attaining the highest peak temperatures.

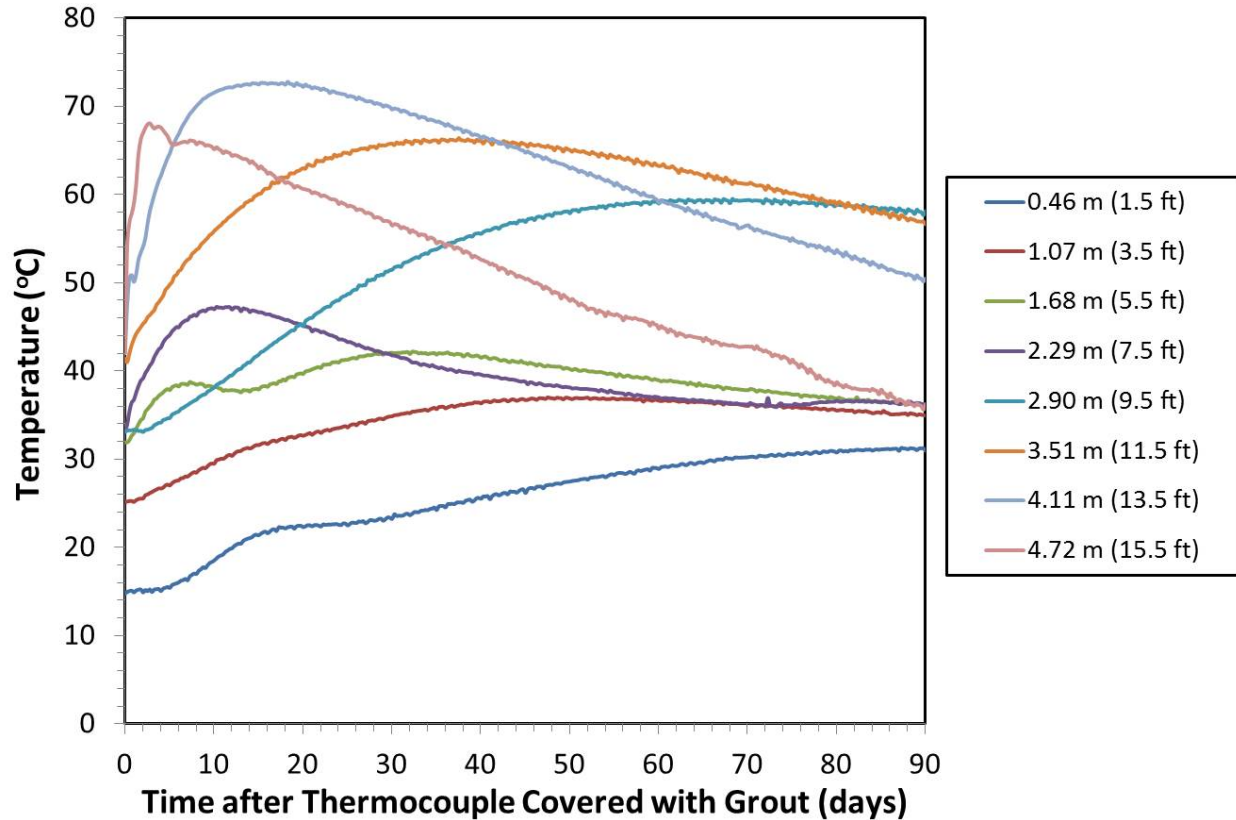


**Figure 5:** Thermocouple outputs for elevations from 0.46 to 4.7 meters (1.5 to 15.5 feet) in an SDU with time zero normalized to the time at which each thermowell was initially covered with grout.

Given the observed variation in thermal history a number of questions arise; (1) do the temperature variations observed significantly affect the post-cured properties (in particular, saturated hydraulic conductivity for the purpose of this discussion), (2) if it is thought that the properties are affected, how large is the effect and is it negative or positive, and (3) at what temperatures should simulant samples be cured in the laboratory to adequately mimic those in the SDU? A discussion of Questions (1) and (2) is considered in the later text, and ultimately determines the relevance of Question (3). However, published data suggest that the curing temperature profile of cementitious materials, including saltstone, does indeed influence the properties of the cured product with the predominance of data suggesting that properties, such as compressive strength and permeability, can be negatively impacted. However, it is important that each study be considered in the context of the thermal regime applied during curing as opposed to merely considering the peak curing temperature. Question (3) simply arises from the fact that it is impractical to conduct curing according to every thermal profile recorded in an SDU, and as such a reduced sub-set of representative thermal profiles that adequately encompass the variable thermal history observed in an SDU is sought. Ideally, identification of a single profile is preferred, though considering Figure 5, it may not be appropriate to apply a single curing temperature regime to represent the thermal history of the entire saltstone monolith. For example, while a room temperature cure could be considered representative of the profiles observed at the 0.46 and 1.07-meter (1.5 and 3.5-foot) elevations, such a temperature profile may not be applicable for simulating the curing (and the resulting properties) of the grout emplaced at the 4.1 meter (13.5-foot) level. Similarly, using a curing temperature regime that mimics the profile at 4.1-meter (13.5-foot) elevation may not be applicable for assessing the properties of material

emplaced in the bottom portion of the SDU, which was subjected to lower curing temperatures. As stated above, determining the appropriate thermal profiles that are representative of the saltstone monolith depends on how the curing process, and the resulting microstructure and properties, are affected by temperature. This is discussed with specific respect to saturated hydraulic conductivity in the subsequent section.

### **EFFECT OF CURING TEMPERAURE ON SALTSTONE SATURATED HYDRAULIC CONDUCTIVITY**

All cementitious materials are inherently porous and therefore permeable. Saturated hydraulic conductivity (which is directly proportional to the permeability for a permeating fluid of given viscosity and density) is a key property of saltstone that is used to model the long-term ingress of oxygen-bearing groundwaters that may ultimately mobilize redox sensitive contaminants, most notably <sup>99</sup>Tc. The currently assumed value of saturated hydraulic conductivity utilized for modeling contaminant transport in the SDF Performance Assessment (PA) is 6.4E-09 cm/sec [3]. While the total porosity in hydrated cement influences the saturated hydraulic conductivity, it is actually the pore size, dispersion, and connectivity that are the key determinants. For example, saltstone has a total porosity of 50-60% yet its saturated hydraulic conductivity is typically measured at around E-09 cm/sec [14-16]. Cementitious materials contain two primary types of pore, namely gel (or interlayer) and capillary pores. Gel pores consist of the interlayer space within the gel structure that forms during hydration, and are a few nanometers in size. As such they do not significantly affect the saturated hydraulic conductivity of the material. Capillary pores are much larger (up to 5 microns) and represent the space in the cured material that is not filled with reaction products. Using the hydration of Portland cement as an example, the primary components of cement are calcium silicates which react with water to produce calcium silicate hydrate (C-S-H) gel and calcium hydroxide. Completely hydrated cement consists of 50 vol% or more C-S-H, and as such this phase has significant influence with respect to the post-cured properties of cement. This influence with respect to saturated hydraulic conductivity is limited not only to the amount of C-S-H produced, but also to the distribution of the material and its ability to fill the capillary pores in the cement and reduce the pore connectivity. As the hydration reactions progress the amount, size, and connectivity of capillary porosity is reduced by the growth of the C-S-H into the pore space; it is this mechanism which ultimately serves as a key determinant with respect to the saturated hydraulic conductivity of cement.

It is also important to remember that saltstone consists of three reactive powder components, namely cement, BFS, and FA. Of these three materials, it is not surprising that most studies regarding the influence of curing temperature have concentrated on Portland cement (though this constitutes only 10 wt% of the saltstone dry feed material). Verbeck et al. [4] suggested that curing at higher temperatures resulted in non-uniform distribution of the hydration products (in particular C-S-H) within the microstructure, with a high concentration of hydration product building up around the hydrating particles and retarding subsequent hydration, while at low temperatures hydration products had sufficient time to diffuse and precipitate more uniformly throughout the cement matrix. Thus, higher temperatures reduced both the amount of reaction product and its ability to diffuse and block off capillary pores. Goto et al. [5] characterized the pore structure and resulting saturated hydraulic conductivity for hardened cement paste samples cured at 27 ° and 60 °C (note that for each temperature samples were initially cured for 1 day at room temperature before being subjected to a 28-day cure at their respective temperatures). At 27 °C the saturated hydraulic conductivity (for a w/c = 0.35) was approximately 4E-09 darcy compared to 1E-07 darcy at 60 °C. When water is the permeating fluid, 1 darcy is equivalent to a hydraulic conductivity of 8.58E-04 cm/sec [6]. The increased saturated hydraulic conductivity for the higher temperature cure occurred despite the fact that this sample had a total porosity of 30% compared to 35% for the lower temperature cure. This was attributed to enhanced dispersion of the reaction products resulting in both reduced pore size and improved blocking of the capillary pores. For the 27 °C curing temperature the pore

size did not exceed 0.15 microns whereas pores as large as 5 microns were observed for the higher temperature cure.

With respect to BFS and FA, while the effect of elevated curing temperatures on the compressive strength of these materials has received some attention, little work has been conducted with respect to the effects on pore volume and distribution, and the subsequent effects on saturated hydraulic conductivity. FA is a pozzolan (a siliceous/aluminous material) obtained as a by-product from the burning of coal. It does not possess any cementitious properties of its own. It does, however, react with calcium hydroxide (formed during cement hydration) or the free hydroxide contained within the salt waste to form an aluminosilicate gel. Similar to the C-S-H gel formed during cement hydration, the aluminosilicate gel would be expected to reduce the amount, size, and connectivity of capillary pores. However, higher hydroxide concentrations than those present in the salt solution are needed to significantly activate the dissolution and reaction of FA [7]. In addition, FA reaction at ambient temperatures is slow [8]. Figure 6 indicates FA particles in a blended material cured at ambient temperatures for 7 and 28 days [9]. After 7 days, no reaction of the FA is discernible. At 28 days the FA reaction is still limited but reaction product is observed as a thin layer around the FA particle.

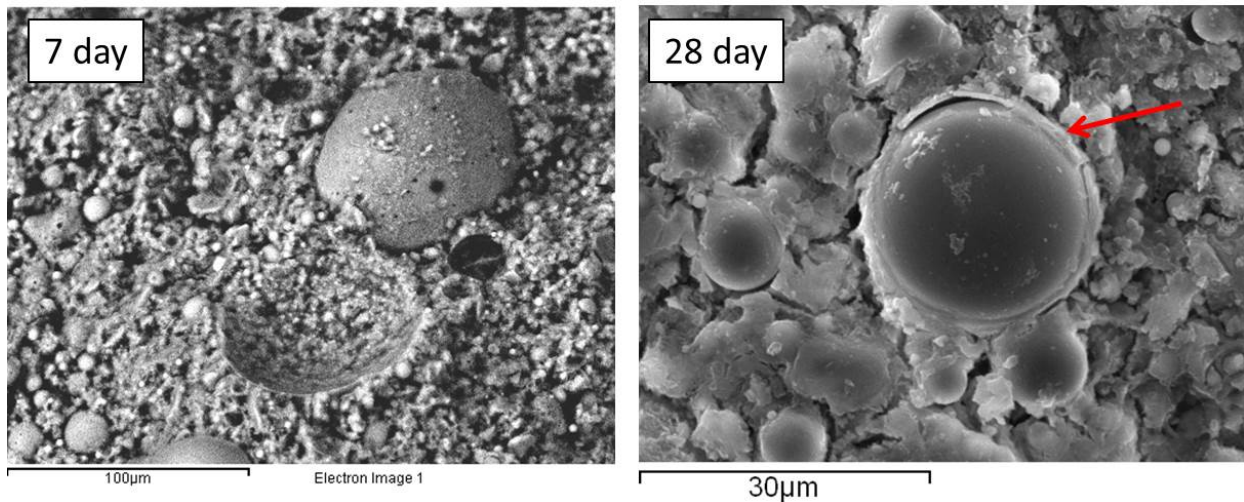


**Figure 6:** Micrographs indicating insignificant reactivity of FA after curing for 7 and 28 days at ambient temperatures [9].

Due to this low reactivity at ambient temperature, higher curing temperatures may actually aid the reactivity of FA. Indeed, a study by Palomo et al. [10] on the alkali activation of FA found that increasing the curing temperature from 45 °C to 65 °C increased the rate of mechanical strength development five-fold while a 10-fold increase was recorded between 65 °C and 85 °C.

BFS is a by-product of iron and steel making and results from the rapid cooling of molten iron slag. The primary components of BFS are calcia, silica, alumina, and magnesia. While BFS will hydrate in the presence of water, its dissolution and subsequent reactivity are enhanced in alkaline environments. Alkali-activated BFS results in the formation of a C-S-H product similar to the gel produced during cement hydration but with a higher aluminum content [11]. Hence it is anticipated that the formation and distribution of this gel will be a key determinant with respect to the pore characteristics and saturated hydraulic conductivity of saltstone. As with FA, the reaction of BFS is enhanced by increased alkali concentration and temperature [12]. With respect to temperature, while increased temperatures accelerated hydration and strength development in the early stages of curing, longer curing durations resulted in an inversion of this relationship, with the ambient cured materials achieving the highest



strengths.

While information regarding the temperature effects on the individual saltstone components is useful, the influence of temperature on the post-cured properties of blended materials may be difficult to predict from this information since the components and their products can both interact and compete. On the one hand, elevated curing temperature of cement would seem to result in less homogeneous pore distribution and greater saturated hydraulic conductivity [6], whereas elevated temperatures may enhance the reactivity and distribution of BFS and FA. Regarding blended materials, a study by Roy et al. [13] indicated that curing temperatures up to 60 °C had little effect on the porosity and pore size distribution for OPC/BFS mixtures, which is contrary to the results for cement alone [6]. In addition, with respect to the effect of curing temperature on the saturated hydraulic conductivity of saltstone, a number of studies have been conducted since it is a key input for long-term performance models. Table 1 provides the primary details on each of the studies including the curing temperature regime and the resulting saturated hydraulic conductivity.

References 14 and 15 (Table 1) indicate a significant effect of elevated temperature curing, though it was acknowledged by the authors that the thermal profiles utilized were not intended to be representative of emplaced saltstone. For both studies, the samples were placed directly into ovens that had been pre-heated to the designated curing temperature. For room temperature cures, the saturated hydraulic conductivity was around 1E-09 cm/sec whereas this increased significantly for all samples cured at 60 and 80 °C for 21 days (1E-06 to 1E-07 cm/sec). Reference 14 also provides values for total porosity and it is noteworthy that the samples cured at room temperature had an average total porosity of 62% in comparison to 64% for samples cured at 60°C. This result is in agreement with the earlier assertion that the total porosity is not the key determinant with respect to sample saturated hydraulic conductivity. Based on the study by Goto et al. [6], it is perhaps probable that the pore size distribution and the pore connectivity are markedly different between the room temperature and the 60 and 80 °C curing temperatures.

In contrast, a study that attempted to mimic temperature profiles recorded in the SDUs (including the ramp to the peak temperatures of 57° and 82 °C) indicated hydraulic conductivities of 3E-09 cm/sec for both peak temperatures after only 28 days of curing [16]. Two additional studies were also aimed at mimicking the temperature profiles in the SDUs [17, 18]. The methodology for Reference 17 was to closely mimic a temperature profile recorded in an SDU whereas for Reference 18 it was to use simplified profiles (based on temperature profiles recorded in the SDU) with a constant starting point of room temperature, constant heating rate of 10 °C per day, and peak temperatures of 35, 45, and 55 °C, followed by hold times to 28 and 90 days of total curing time. The latter study was designed to provide a sub-set of thermal profiles that would encompass the thermal history observed in an SDU. For Reference 17, the 28-day hydraulic conductivity was initially measured at 3E-08 cm/sec but decreased to 5E-09 cm/sec with extended 90-day curing. For Reference 18, saturated hydraulic conductivities at 28 days were in the range of 2 to 5E-09 cm/sec, while at 90 days they ranged between 1 to 2E-09 cm/sec for all curing temperatures.

Decreased hydraulic conductivity for a 90-day cure in comparison to a 28-day cure was also observed for References 19 and 20, which utilized equivalent saltstone simulant compositions and curing temperature profiles to those used in Reference 17. Twenty-eight day saturated hydraulic conductivities were measured at 2E-8 cm/sec [19] and 7E-09 cm/sec [20]. After 90 days of curing the saltstone simulant indicated a hydraulic conductivity of 2E-09 cm/sec [20].

Thus, it appears that while isothermal curing to between 60-80 °C in a pre-heated oven results in increased saturated hydraulic conductivity (at least with respect to shorter term curing), the incorporation of a ramp to the peak temperature results in similar hydraulic conductivities to those measured for ambient cured materials; this is particularly the case for samples cured for 90 days. It is thus likely that in the first few days of curing, temperature plays a critical role in the reaction kinetics, product formation, and microstructure/pore development. Higher temperatures may lead to rapid product formation that

subsequently inhibits the continued reaction/hydration of the dry feed materials. However, there is also evidence to suggest that longer curing times normalize the degree of hydration and resultant properties irrespective of the peak curing temperature.

### **OTHER FACTORS AFFECTING SALTSTONE PROPERTIES**

While it is possible to mimic the environmental conditions (temperature and humidity) in an SDU, there are still aspects of the process not readily simulated in the laboratory but which may significantly influence the ultimate properties of saltstone actually emplaced in the SDU. These may include differences with respect to field and laboratory mixing, the action of pumping the grout in the field along varying pipe lengths and then dropping it into the SDU, and the action of grout spreading from the pour location to the extremities of the SDU. More recent endeavors have been aimed at simulating these process characteristics in laboratory-prepared samples. Most notable is the use of the Scaled Continuous Processing Facility (SCPF) developed at Savannah River National Laboratory (SRNL). The SCPF was developed by SRNL to complement traditional small-scale laboratory testing of saltstone and to provide processing that more closely simulates actual SPF operations including the use of a high shear mixer, mixer discharge hopper, peristaltic pump, and transfer lines. In 2013, 700 gallons of saltstone simulant was prepared utilizing the SCPF and poured into a B-25 container (1.83 meters (L) x 1.22 meters (W) x 1.22 meters (H)) (6 feet (L) x 4 feet (W) x 4 feet (H)) (Figure 7). This was used as a mock-up for the future core-drilling of samples from an SDU [21]. Of note is the fact that samples extracted from approximately 0.3 meters (1 foot) below the monolith surface (after 60 days of curing) indicated saturated hydraulic conductivities of  $2E-09$  cm/sec, similar to those values for samples subjected to curing temperature regimes representative of the SDUs [16-20]. Though the temperature history of these samples is not known it is fair to assume that they were subjected to temperatures above ambient (noting that the B-25 was positioned outside from mid-June to mid-August prior to sample drilling) as a result of the heat evolved during grout hydration and the insulating effects of the surrounding material. Indeed, a similar sized monolith fitted with thermowells and filled with Cast Stone [22] (the cementitious material being considered for immobilizing Low Activity Waste (LAW) at the Hanford Site) indicated internal temperatures that rose from ambient to 70 °C in a 5 day period, followed by a few days hold around the peak temperature, and subsequent reduction in temperature to around 45 °C in approximately 8 days. A similar profile could therefore be expected for grout curing in the center of the aforementioned (and similarly sized) B-25 monolith [21].

### **SUMMARY**

The main intent of this paper was to consider data derived from curing saltstone in simulated field environments in the laboratory to determine the degree to which the temperature profile influences the post-cured properties, in particular saturated hydraulic conductivity, and to establish the most appropriate curing regimes to simulate field conditions. Temperature and humidity profiles have both been measured in an SDU and these two parameters are easily controlled in the laboratory. However, while the RH% in an SDU typically ranges 95-100%, the temperatures associated with grout curing vary considerably with respect to starting temperature, peak temperature (and duration at the peak temperature), and heating/cooling rates. Thus, questions arise as to whether the variation in curing regimes to which the saltstone is subjected adversely affect key properties, specifically saturated hydraulic conductivity with respect to this discussion, and if so, what curing temperature regimes should be used in the laboratory to adequately simulate an array of field conditions.

Saltstone consists of three reactive components, namely Portland cement, BFS, and FA. While data exist with respect to the effect of curing temperature on these individual components, these data may not adequately predict the influence of similar temperature regimes on the combination of the three materials due to inter-reaction and competition, in particular with respect to the consumption of water. A number of studies regarding the influence of curing temperature on saltstone performance have been conducted at

several different laboratories. Those samples that were cured according to an observed SDU temperature profile (and incorporated a ramping of temperature from the initial value to the peak temperature over a period of days) indicated saturated hydraulic conductivities in the range 1-5E-09 cm/sec. In some cases higher values of hydraulic conductivity (E-08 cm/sec) were initially observed for samples cured for 28 days, but lower values (5E-09 cm/sec) were realized after curing for 90 days. Samples cured at elevated temperatures without incorporating the characteristic thermal ramp indicated hydraulic conductivities in the range of E-06 cm/sec, though it is important to note that these samples were cured for 21 days. It is conceivable that the high initial temperatures provided enhanced reaction kinetics but resulted in the buildup of products that ultimately impeded the homogeneous dispersion of the reaction products throughout the structure, thereby resulting in larger, connected pore networks. It is suspected, however, that continued curing would have resulted in additional product formation and dispersion and ultimately reduced hydraulic conductivity.

In conclusion, this paper confirms the importance of utilizing field-derived environmental data to simulate the curing of saltstone in the laboratory. The curing temperature for the first few days is likely critical with respect to reactivity and microstructure development, and incorporation of characteristic heating ramps observed in all profiles within an SDU is important in producing simulant samples that are comparable in microstructure and properties to field-emplaced samples. It is also conceivable that prolonged curing (>90 days) will result in normalization of saltstone microstructures and properties (irrespective of the curing regime), and this may constitute an area of future study.

## REFERENCES

1. Bannochie, C.J., *Results for the First Quarter 2014 Tank 50 WAC Slurry Sample: Chemical and Radionuclide Contaminants*, SRNL-STI-2014-00203, Rev. 0, May 2014.
2. Mehta, P.K and Monteiro, P.J.M., *Concrete: Microstructure, Properties, and Materials*, 3<sup>rd</sup> Edition, McGraw-Hill (2006).
3. *FY2013 Special Analysis for the Saltstone Disposal Facility at the Savannah River Site*, SRR-CWDA-2013-00062, Rev. 0, Savannah River Remediation LLC (2013).
4. Verbeck, G.J. and Helmuth R.A., *Structures and Physical Properties of Cement Paste*, Proceeding of the 5<sup>th</sup> International Symposium on the Chemistry of Cement, 1-32, Tokyo, 1968.
5. Goto, S, and Roy, D.M., *The Effect of W/C Ratio and Curing Temperature on the Permeability of Hardened Cement Paste*, Cement and Concrete Research, 23, 575-579 (1981).
6. West, T.R., *Geology Applied to Engineering*. Prentice Hall, 560 pp.
7. Somna, K., Jaturapitakkul, C., Kajitvichyanukul, P., and Chindaprasirt, P., *NaOH-Activated Ground Fly Ash Geopolymer Cured at Ambient Temperature*, Fuel, 90, 2118-2124 (2011).
8. Puertas, F., Martinez-Ramirez, S., Alonso, S., and Vazquez, T., *Alkali-Activated Fly Ash/Slag Cement: Strength Behavior and Hydration Products*, Cement and Concrete Research, 30, 1625-1632 (2000).
9. Papathanassiou, A.E., Gong, W., and Pegg, I.L., *Development of Cement-Free Saltstone Formulations Phase 1*, VSL-12R2420-1, Rev. 0, December 2012.
10. Palomo, A., Alonso, S., Fernandez-Jimenez, A., Sobrados, I., and Sanz, J., *Alkaline Activation of Fly Ashes: NMR Study of the Reaction Products*, Journal of the American Ceramic Society, 87 [6] 1141-1145 (2004).
11. Pacheco-Torgal, F., Castro-Gomes, J., and Jalali, S., *Alkali-Activated Binders: A Review: Part 2. About Materials and Binders Manufacture*, Construction and Building Materials, 22 [7] 1315-1322 (2008).

12. Bakharev, T, Sanjayan, J.G., and Cheng, Y.-B., *Effect of Elevated Temperature Curing on Properties of alkali-Activated Slag Concrete*, Cement and Concrete Research, 29, 1619-1625 (1999).
13. Roy, D.M. and Parker, K.M., *Microstructures and Properties of Granulated Slag – Portland Cement Blends at Normal and elevated Temperatures*, 1<sup>st</sup> International Conference on the Use of Fly Ash, Silica Fume, Slag, and Other Mineral By-Products in concrete, Montebello, Canada, ACI Journal, 79, 397-414 (1983).
14. Dixon, K., Harbour, J., and Phifer, M., *Hydraulic and Physical Properties of ARP/MCU Saltstone Grout*, SRNL-STI-2009-00419, Rev. 0, May 2010.
15. Harbour, J.R. and Williams, M.F., *Impact of Curing Temperature on the Saturated Liquid Permeability of Saltstone*, SRNL-STI-2010-00745, Rev. 0, February 2011.
16. Reigel, M.M., Pickenheim, B.R., and Daniel, W.E., *Process Formulations and Curing Conditions that Affect Saltstone Properties*, SRNL-STI-2012-00558, Rev. 0, September 2012.
17. Papathanassiou, A.E., Gong, W., Xu, H., McKeown, D., and Pegg, I.L, *Oxidation Rate Measurement and Humidity Effects on Saltstone*, VSL-13R3010-1, Rev. 0, August 2013.
18. Papathanassiou, A.E., Gong, W., Xu, H., Buechele, A.C., and Pegg, I.L, *Saltstone Curing Assessment*, VSL-14R3310-1, Rev. 0, February 2014.
19. Seaman, J.C., Chang, H.-K., and Buettner, S.W., *Comparison of Hydraulic Property Measurement Techniques for Simulated Saltstone*, SREL Doc. R-13-0006, Ver. 1.0, September 2013.
20. Seaman, J.C., Chang, H.-K., and Buettner, S.W., *Chemical and Physical Properties of Saltstone as Impacted by curing Duration*, SREL Doc. R-14-0006, Ver. 1.0, September 2014.
21. Simner, S.P., *Physical Property Comparison of Core-Drilled and Cast Simulant Saltstone*, SRR-SPT-2013-00056, Rev. 0, March 2014.
22. Cozzi, A.D., Fowley, M.D., Hansen, E.K., Eibling, R.E., Fox, K.M., Miller, D.H., and Williams, M.R., *Engineering Scale Demonstration of a Prospective Cast Stone Process*, SRNL-STI-2014-00428, Rev. 0, September 2014.

**Table 1:** Saturated hydraulic conductivities of saltstone exposed to varied curing temperature regimes.

Peak Temp. (°C)	Temperature Profile	Total Curing Duration (days)	Avg. Saturated Hydraulic Conductivity (cm/sec)	Reference (Year) [Ref.]
RT	RT for 28 days	28	1E-09	SRNL-STI-2009-00419 (2009) [14]
60	60 °C for 28 days	28	8E-07	
RT	RT for 30 days	30	1E-08	SRNL-STI-2010-00745 (2010) [15] <sup>3</sup>
40	40 °C for 21 days <sup>1</sup>	21	1E-06	
60	60 °C for 21 days <sup>1</sup>	21	1E-06	
80	80 °C for 21 days <sup>1</sup>	21	1E-06	
RT	RT for 30 days	30	1E-09	SRNL-STI-2010-00745 (2010) [15] <sup>4</sup>
40	40 °C for 21 days <sup>1</sup>	21	1E-09	
60	60 °C for 21 days <sup>1</sup>	21	1E-07	
80	80 °C for 21 days <sup>1</sup>	21	1E-06	
57 <sup>2</sup>	RT → 57 °C in 5 days 57°C → 45 °C in 23 days	28	3E-09	SRNL-STI-2012-00558 (2010) [16]
82 <sup>2</sup>	RT → 57 °C in 5 days 57°C → 82 °C in 23 days	28	3E-09	
65 <sup>2</sup>	45 °C → 65 °C in 26 days Hold at 65 °C for 2 days	28	3E-08	VSL-13R3010-1 (2013) [17]
65 <sup>2</sup>	45 °C → 65 °C in 26 days Hold at 65 °C for 10 days 65 °C → 59 °C in 24 days	60	4E-09	
65 <sup>2</sup>	45 °C → 65 °C in 26 days Hold at 65 °C for 10 days 65 °C → 52 °C in 54 days	90	5E-09	

<sup>1</sup> Information not provided in reference but details provided in communication with SRNL staff.

<sup>2</sup> Samples subjected to thermal profiles representative of actual SDUs.

<sup>3/4</sup> Data from Reference \* for saltstone samples prepared using low<sup>3</sup> and high<sup>4</sup> aluminate concentration in for salt solution.

<sup>5</sup> Two sample sets prepared at SREL; 1<sup>st</sup> set tested at SREL; 2<sup>nd</sup> set tested at AMEC.

**Table 1 (cont.):** Saturated hydraulic conductivities of saltstone exposed to varied curing temperature regimes.

<b>Peak Temp. (°C)</b>	<b>Temperature Profile</b>	<b>Total Curing Duration (days)</b>	<b>Avg. Saturated Hydraulic Conductivity (cm/sec)</b>	<b>Reference (Year) [Ref.]</b>
65 <sup>2</sup>	45 °C → 65 °C in 26 days Hold at 65 °C for 2 days	28	2E-08 <sup>5</sup>	SREL Doc. R-13-0006 (2013) [19]
65 <sup>2</sup>	45 °C → 65 °C in 26 days Hold at 65 °C for 4 days	30	7E-09	SREL Doc. R-14-0006 (2014) [20]
65 <sup>2</sup>	45 °C → 65 °C in 26 days Hold at 65 °C for 10 days 65 °C → 52 °C in 54 days	90	2E-09	
35	RT → 35 °C in 1 day Hold at 35 °C	28	5E-09	VSL-14R3210-1 (2013) [18]
		90	2E-09	
45	RT → 45 °C in 2 days Hold at 45 °C	28	2E-09	
		90	2E-09	
55	RT → 55 °C in 3 days Hold at 55 °C	28	2E-09	
		90	1E-09	

<sup>1</sup> Information not provided in reference but details provided in communication with SRNL staff.

<sup>2</sup> Samples subjected to thermal profiles representative of actual SDUs.

<sup>3/4</sup> Data from Reference \* for saltstone samples prepared using low<sup>3</sup> and high<sup>4</sup> aluminate concentration in for salt solution.

<sup>5</sup> Two sample sets prepared at SREL; 1<sup>st</sup> set tested at SREL; 2<sup>nd</sup> set tested at AMEC.